

INTERACTIONS BETWEEN SNOW METAMORPHISM AND CLIMATE: PHYSICAL AND CHEMICAL ASPECTS

F. Domine^{1*}, A.-S. Taillandier¹, S. Houdier¹, F. Parrenin¹, W.R. Simpson² and Th.A. Douglas³

¹CNRS, Laboratoire de Glaciologie et Géophysique de l'Environnement, BP 96, 38402 Saint-Martin d'Hères Cedex, France. *E-mail : florent@lgge.obs.ujf-grenoble.fr

²Geophysical Institute, University of Alaska Fairbanks, Fairbanks, Alaska, USA, and Department of Chemistry, University of Alaska Fairbanks, USA

³Cold Regions Research and Engineering Laboratory, Fort Wainwright, Alaska, USA.

1 INTRODUCTION

The snowpack forms an interface between the atmosphere and the ground or sea ice that affects the energy balance of the Earth's surface^{1,2} and the exchange of chemical species between the surface and the atmosphere.³ Studies of snow areal extent (e.g. ref. 4) show that during the boreal winter snow covers about 14% of the Earth's surface, therefore affecting the surface energy balance at near-planetary scales, while its overall effect on tropospheric chemistry still needs to be assessed.

The physical impact of the snowpack depends on its physical properties, such as albedo and heat conductivity. Its chemical impact depends on its chemical composition and its reactivity, determined in part by the light flux inside the snowpack. All of these properties change with time, because of a set of physical and chemical processes regrouped under the term "snow metamorphism", defined below.

Snow is a porous medium formed of air, ice crystals and small amounts of chemical impurities. Because ice has a high vapor pressure (165 Pa at -15°C, 610 Pa at 0°C), the vertical temperature gradient that is almost always present within the snowpack generates sublimation and condensation of water vapor that change the size and shape of snow crystals. This results in changes in physical variables such as density, albedo, heat conductivity, permeability and hardness. These physical changes have formed the basis for the definition of snow metamorphism.⁵

Interest has recently developed in snowpack compositional changes associated with metamorphism. Motivation includes the interpretation of chemical analyses of ice cores⁶ and the understanding of the impact of the snowpack on tropospheric chemistry.³ Indeed, sublimation and condensation of water vapor entrains trace gases dissolved within ice crystals, which has been invoked to explain concentration changes of species such as HCl, HNO₃, HCHO and H₂O₂.⁷⁻¹⁰ The light that penetrates inside the snowpack¹¹ also drives photochemical reactions^{12,13} resulting in changes in snow chemical composition. The growing documentation of these chemical changes during metamorphism imposes their

consideration as a new aspect of snow metamorphism. We therefore propose to define “physical metamorphism” as “the changes in physical properties undergone by snow after deposition” while “chemical metamorphism” can be defined as “the changes in chemical composition undergone by snow after deposition”.

Next to the temperature gradient inside the snowpack, an important driving force for snow metamorphism is wind, that lifts, transports and redeposits snow crystals, changing snowpack mass and density^{14,15} and deposits aerosols inside the snowpack.^{16,17} Wind and temperature are climatic variables that determine metamorphism and snowpack physical properties such as albedo and heat conductivity. These properties affect the energy balance of the snow-atmosphere and of the soil-snow interfaces, which in turn affect climate.

Snow-climate feedbacks therefore exist. The most discussed is probably the snow areal extent–climate feedback⁴, as a reduced snow cover caused by warming changes the surface albedo from high to low values, exerting a positive feedback. Predicted increases in soot deposition to snow are also expected to decrease snow albedo, constituting another positive feedback.¹⁸ Changes in vegetation patterns in the Arctic may also produce complex feedbacks. For example, warming-induced shrub growth on the tundra will trap snow, limit the effect of wind and this will result in snow with a lower heat conductivity.¹⁹ The soil temperature will therefore rise, leading to increased shrub growth and increased emissions of CO₂, a greenhouse gas, by the soil due to enhanced microbial activity. While this snow-vegetation interaction may produce a positive feedback, very complex effects are involved, so that its sign and magnitude are uncertain, as detailed in Sturm et al.¹⁹

Snowpack chemical emissions include oxidants and aerosol precursors, that also interact with climate. Oxidants determine the lifetime of greenhouse gases and aerosols impact the atmospheric radiation budget.²⁰ If snowpack chemical emissions are determined by climate, feedback loops involving snow chemistry also need to be studied to assess the extent of climate change in snow-covered regions.

The purpose of this paper is to reflect upon the existence of feedback loops between climate and snow metamorphism, both physical and chemical. Snow metamorphism has been much studied (e.g. refs. 5,21-23) and we present a brief reminder to feed our discussion. We first recall how climate affects snow physical properties by discussing the major seasonal snowpack types. We then explain the role of temperature and wind speed in the formation of these types. We then focus on four important snowpack variables : albedo, light penetration, heat conductivity, air permeability, and discuss how climate change will affect these variables. Attempts to quantify snow-climate feedbacks are made for some of these properties. Finally, we discuss how physical changes in snowpacks may affect changes in snow chemical composition. Snow-climate feedbacks are extremely complex and quantifying them, or even just determining their sign, will require much further research. However, we wish to put forward ideas to stimulate discussion and this will require making some highly speculative propositions that will need further testing.

A further limitation of this paper is that it focuses on dry metamorphism, i.e. in the absence of melting. Melting obviously affects snowpack physics and chemistry in an important manner and some limited discussion of its impact will nevertheless be included here, but detailed considerations of these additional aspects will require a separate paper.

2 BACKGROUND

Among several existing classifications of seasonal snowpacks, we use that of Sturm et al.²⁴ that describes the tundra, taiga, Alpine, maritime, prairie and ephemeral snowpacks. Sturm et al. also mention the mountain snowpack, that displays such large spatial variations that it

defies a precise definition. The ephemeral snowpack affects only episodically temperate areas and has a limited long-term effect. It will not be discussed. The prairie snowpack covers the Asian steppe and North-American grasslands. Its impact is limited because it is often spatially and temporally discontinuous. We therefore limit our discussions to the taiga, tundra and maritime/Alpine snowpacks, these last two types presenting sufficient similarities to be discussed together.

2.1 The taiga snowpack

The Taiga snowpack covers cold forested regions in North America and Eurasia, as represented in detail in Sturm et al.²⁴ It is typically 50 cm thick (Figure 1) and covers the ground from October-November to April. In mid-winter, it is composed of a thick basal layer formed of centimetric depth hoar crystals, that has a very low mechanical strength, and a density near 0.2 g.cm^{-3} . It is topped by a layer of faceted crystals 1 to 2 mm in size, that eventually transform into depth hoar.²² Layers of decomposing crystals and of fresh snow are observed after snow falls. All of these snow layers have a low density, typically $< 0.2 \text{ g.cm}^{-3}$ as shown in Figure 1.

In these forested and mostly inland areas, wind speed remains low, typically below 2 m.s^{-1} . Winter temperatures frequently drop below -30°C , while ground temperatures remain above -10°C and the temperature gradient has a typical value of $50^{\circ}\text{C.m}^{-1}$. In the fall, the combination of cold spells and of a thin snow cover can raise the temperature gradient to 100, even $200^{\circ}\text{C.m}^{-1}$.²²

2.2 The tundra snowpack

The tundra snowpack covers cold treeless regions around the Arctic ocean and treeless parts of central Asia, south of the taiga region. It is typically 40 cm thick (Figure 1) and covers the ground from September-October to June in the Arctic. In mid-winter, it is composed of a basal layer of centimetric depth hoar crystals of density 0.25 to 0.35 g.cm^{-3} . It is topped by a hard to very hard layer of small wind-packed rounded grains 0.2 to 0.3 mm in size, of density 0.35 to 0.55 g.cm^{-3} .²⁵ Near the surface, recent snowfalls transform into faceted crystals and eventually into depth hoar in the absence of wind. If they are wind-blown, the crystals are then broken up and sublimate while air-borne,¹⁵ contributing to the build-up of the windpack layer.

In these unforested and mostly coastal areas, wind speeds reach values up to 15 to 35 m.s^{-1} . Winter temperatures often drop below -35°C and the longer snow season, coupled to a higher heat conductivity of the snow than on the taiga, contributes to an efficient ground cooling that limits the value of the temperature gradient to typical values of 15 to $40^{\circ}\text{C.m}^{-1}$, except in the fall, when the snowpack is thin and the ground still near 0°C .

2.3 The maritime and Alpine snowpacks

The maritime and Alpine snowpacks are found in temperate regions with abundant precipitation and reach thicknesses of 1 to 2 m, sometimes much more. They cover the ground from November-December to March-May. An example of maritime snowpack stratigraphy is shown in Figure 1. The warm climate results in numerous periods when the temperature exceeds 0°C . The resulting snow melting and subsequent refreezing forms layers of ice and of melt-freeze polycrystals, resulting in an overall density of the base of the snowpack around 0.4 g.cm^{-3} . These layers, when frozen, are mechanically very strong. In the absence of melting, fresh snow transforms into small rounded grains, that form most

of the snowpack. Melting events happen at any time of the year. When sufficient liquid water forms, percolation takes place. Upon refreezing, horizontal ice layers and vertical ice columns (percolation channels) form in the snowpack.

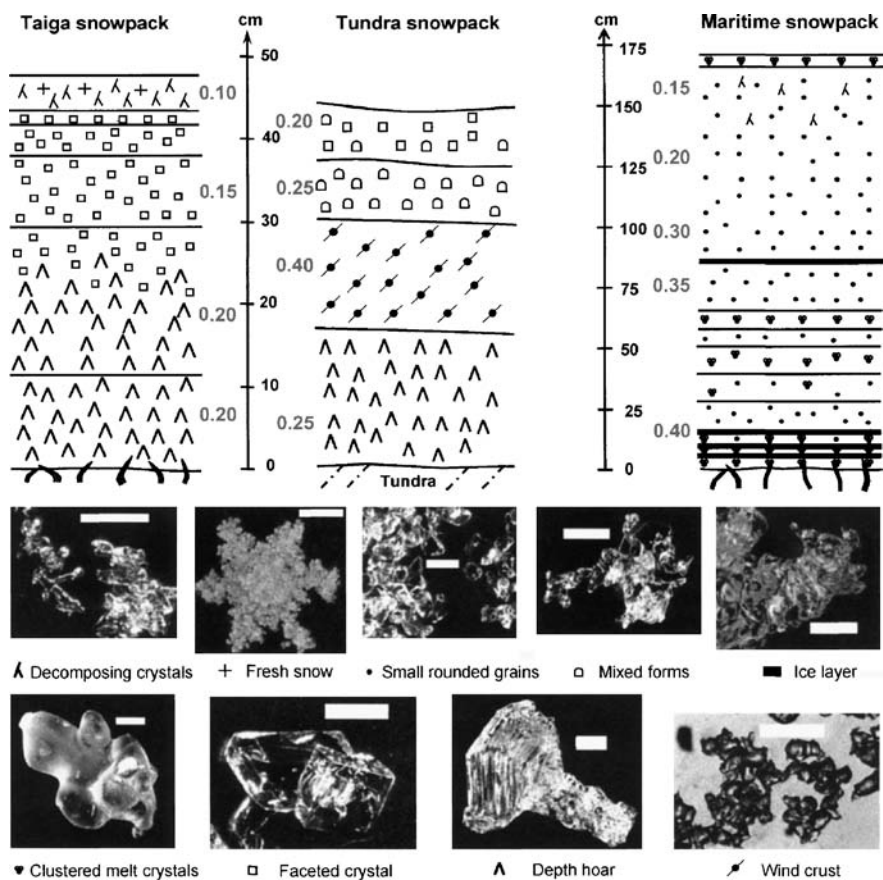


Figure 1 Typical stratigraphies of the taiga, tundra and maritime snowpacks, with photomicrographs of typical snow crystal types. Scale bars: 1 mm. Bold numbers next to the stratigraphies are density values, in g.cm^{-3} .

Temperate maritime areas are usually forested, resulting in low wind speeds. The mild temperatures, combined with a thick snowpack, lead to a very low temperature gradient, of the order of 2 to $5\text{ }^{\circ}\text{C.m}^{-1}$, except near the surface, where daily temperature variations can lead to elevated transient gradients that change sign during the day. The density of the maritime snowpack usually increases monotonously with depth.

The Alpine and maritime snowpacks have many similarities. A specific figure is not necessary here and can be found in Sturm et al.²⁴ Alpine snowpacks form in regions slightly colder than the maritime snowpack and signs of melting are less frequent. The temperature gradient in late fall can be sufficient to form a depth hoar layer 5 to 20 cm

thick. With sufficient snowpack build-up, however, typical gradient values are 5 to 10 $^{\circ}\text{C.m}^{-1}$. The Alpine snowpack forms in regions with little vegetation and windpacks can be found. Overall, the density increases with depth, but not as monotonously as in the maritime case. The basal depth hoar layer, when present, has a density between 0.25 to 0.30 g.cm^{-3} , and windpacks can be denser than underlying layers not affected by wind.

2.4 Temperature and snow metamorphism

Dry metamorphism operates by the transfer of water vapor between ice surfaces, caused by a gradient in water vapor pressure. The vapor pressure over an ice surface is determined by temperature following Clapeyron's law and by the curvature of the surface following Kelvin's law. A snow crystal located in a layer at -12°C within a temperature gradient of $20^{\circ}\text{C.m}^{-1}$ is subjected to a gradient in water vapor pressure of 5 Pa.m^{-1} . In an isothermal snowpack at -12°C , the gradient in water vapor pressure will be determined solely by differences in curvature. Radii of curvature for fresh snow crystals are of the order of 10 μm for sharp edges^{23,26} and 1000 μm for flat faces. For a crystal 4 mm in size, the resulting gradient between a sharp angle and a flat face will be 0.2 Pa.m^{-1} , illustrating that the greatest water vapor fluxes will be found when high temperature gradients are present.

At the beginning of the snow season, ground temperatures are usually close to 0°C , so that the temperature gradient is determined by the atmospheric temperature. In temperate areas with a maritime or Alpine snowpack, the temperature gradient will usually be less than $10^{\circ}\text{C.m}^{-1}$, while in subarctic or Arctic areas, it will usually be greater than $20^{\circ}\text{C.m}^{-1}$.

Under high temperature gradient (typically $>20^{\circ}\text{C.m}^{-1}$,²⁷), high water vapor fluxes lead to rapid crystal growth producing large faceted crystals with sharp edges, becoming hollow as size increases.²¹⁻²³ These large hollow faceted crystals can reach several cm in size and are called depth hoar crystals. No preferential growth takes place at grain boundaries and layers of faceted or depth hoar crystals are highly uncohesive and their presence considerably increases the avalanche risk in mountain areas.²⁸ This intense metamorphism is hereafter called high gradient metamorphism (HGM).

Under low temperature gradient (typically $<10^{\circ}\text{C.m}^{-1}$), crystal growth is too slow to lead to the formation of large faceted crystals.²³ The curvature dependence of the water vapor pressure has an effect : highly positively curved (convex) areas sublimate while condensation takes place on flat and concave areas. This process leads to rounded crystals that form cohesive layers because concavities exist at grains boundaries, that grow preferentially. Growth being slow, crystals remain small, typically 0.5 mm or less. This low-intensity metamorphism is hereafter called quasi-isothermal metamorphism (QIM).

The impact of the temperature gradient on metamorphism explains many of the features of Figure 1. The typical HGM-type metamorphism of the taiga snowpack eventually transforms most of the snowpack into depth hoar,²² while the QIM-type metamorphism of the maritime and Alpine snowpacks forms, in the absence of melting, layers of small rounded grains 0.2 to 0.4 mm in diameter. However, considering the effects of other climate variables such as wind speed is necessary to explain features such as the presence of windpacks formed of small rounded grains in the tundra snowpack.

2.5 Wind and snow metamorphism

Wind of moderate speed can drag snow crystals on the surface, or lift them so that they undergo saltation or become suspended in air.¹⁴ Saltation, i.e. bouncing and breaking on the snow surface, leads to grain fragmentation and sublimation²⁹ and crystals are usually 0.1 to 0.3 mm in diameter. Crystals accumulate in wind-sheltered areas, such as the lee of

sastrugi^{15,25} and form dense layers of small grains, mostly rounded. (Sastrugi are small dune-like structures 5 to 30 cm high formed by deposition/erosion processes during wind storms²⁵). The density of windpacks thus formed depends on wind speed and may exceed 0.5 g.cm^{-3} for wind speeds greater than 20 m.s^{-1} .

In dense windpacks, crystals do not appear to have the space required to grow to large sizes and this has been invoked to explain why depth hoar does not grow in dense snow.²⁷ However, we found depth hoar of density up to 0.4 g.cm^{-3} on the tundra, so that space is probably not the only factor. As detailed below, windpacks have a high heat conductivity that hinders the establishment of a high temperature gradient across them and this may also explain why little transformation is observed in such snow layers.

In the absence of wind, snow density increases because of loading by subsequent layers and of destruction of small structures by sublimation, leading to the collapse of crystals higher up. Without wind and melting and under QIM conditions, snow density is around 0.35 g.cm^{-3} at 1 m depth. Under HGM conditions, compaction is compensated by upward vapor fluxes,²² limiting the density of basal depth hoar layers to about 0.2 g.cm^{-3} .

3 PHYSICAL PROPERTIES OF THE SNOWPACK

3.1 Selection of variables

Variables such as density, albedo, light e-folding depth, specific surface area (SSA), crystal size and shape, heat conductivity, permeability, diffusivity and shear resistance are required for a complete physical description of the snowpack. Not all these variables have major relevance to climatic issues. Albedo, i.e. the fraction of incident light that is reflected, has obvious climatic relevance and is discussed here. It depends in part on crystal size and shape and this dependence can in fact more simply be related in part to the SSA of the snow³⁰ i.e. the surface area accessible to gases per unit mass.³¹

The incident light that penetrates the snowpack undergoes multiple reflections, to the point that a few cm down, the actinic flux can be up to 4 times as large as the incident flux. This amplification is strongly dependent on the solar zenith angle and is greater when the sun is higher on the horizon.¹¹ Below that surface region, the actinic flux decreases exponentially and the snow depth over which the flux decrease by a factor of e is called the e-folding depth. Similarly to the albedo, the e-folding depth depends on snow SSA. Hence, we discuss snowpack albedo, e-folding depth and SSA as a single section.

The second physical variable of obvious climatic relevance is the heat conductivity, that determines the heat flux between the atmosphere and the ground or sea ice. Another section is therefore devoted to this variable.

Snowpack permeability determines air flow within the snowpack, as driven by differences in surface pressure between different parts of the snow surface. Air flow through the snow leads to the exchange of heat and of chemical species between the snow and the atmosphere and is the last physical variable discussed here.

3.2 Albedo, e-folding depth and specific surface area

Snow reflects light at all visible wavelengths and pure snow has an albedo in the visible and near UV in the range 0.96 to 0.98.³² In the IR, snow albedo is much lower, decreasing to values below 0.1 around 1500 and 2000 nm, so that the albedo of pure small-grained snow averaged over the solar spectrum is of the order of 0.8.³³

The interaction of light with snow is described by the combination of two processes : scattering by the numerous surfaces offered by snow crystals and absorption by ice and impurities contained in the snow, such as particles of soot and of mineral dust.^{32,34} These processes are quantified by the coefficients S_c (for scattering) and K (for absorption), both in units of inverse length. Numerous theories with various degrees of sophistication have been proposed to describe light-snow interactions. With sufficiently sophisticated theories,^{35,36} it is possible to relate S_c and K to snow physical properties and chemical composition. Specifically, the scattering coefficient is related to snow SSA and the absorption coefficient is related to the wavelength-dependent absorption of ice and to absorption caused by impurities. Grenfell and Warren³⁷ and Neshyba et al.³⁸ recommend the use of independent spheres with the same surface area-to-volume ratio, S/V , as a non-spherical ice crystal for calculating optical parameters. This S/V ratio is closely related to the specific surface area (SSA) of snow : $SSA = S/(V \cdot \rho)$ where ρ is the density of pure ice and therefore the scattering coefficient of snow should be related to snow SSA.

Recent developments to measure snow SSA³¹ have allowed the testing of the relationship between SSA and optical properties. In the visible and UV, snow albedo is very high, so that the sensitivity to snow SSA is not large. In the IR this sensitivity is large and Domine et al.³⁰ have recently established a quasi-linear relationship between SSA and snow albedo in the wavelength range 1650-2260 nm. Likewise, Simpson et al.³⁹ observe a proportionality between the optical scattering coefficient of snow and its SSA.

Modeling light-snow interactions will thus use as basic data snow SSA and absorption coefficients by ice and impurities. Our goal is to discuss the modifications of light-snow interactions induced by climate change. Ice absorption is an intrinsic property insensitive to climate. The amount of impurities in snow will be affected by climate, through complex effects on emissions, atmospheric chemical transformations, large scale transport and deposition processes, that are beyond our scope. We instead focus on the physical aspect, i.e. on how climate will affect light scattering by snow and therefore snow SSA.

Most snow SSA values were obtained by measuring the adsorption isotherm of methane on snow at 77 K.³¹ For dry snow, values range from around 1500 cm².g⁻¹ for fresh dendritic snow to about 100 cm².g⁻¹ for depth hoar. Melting severely decreases SSA and values of 18 cm².g⁻¹ have been measured for melt-freeze crusts.⁴⁰

The grain growth almost always observed during metamorphism results in a decrease in snow SSA. The rate of decrease greatly affects snow albedo and e-folding depth, considered over large spatial and temporal scales. The initial decrease is very fast, with a factor of 2 decrease in 1 to 2 days. Experimental and field studies have quantified the rate of decrease of snow SSA as a function of temperature and temperature gradient.⁴¹⁻⁴⁵ In all cases, the best empirical fit of SSA decay plots was of the form :

$$SSA = B - A \ln(t + \Delta t) \quad (1)$$

where t is time and A , B and Δt are adjustable parameters. Several attempts have been made recently to establish a physical basis for these equations^{44,46,47} and it was shown that the rate of isothermal SSA decrease followed the laws of Ostwald ripening. However, the approximations that had to be made render the applicability of these equations highly uncertain. In particular snow crystals were approximated as spheres and Legagneux and Domine⁴⁶ have shown that this resulted in huge errors in SSA estimations. It must therefore be concluded that there is today no reliable theoretical basis to predict the evolution of snow SSA and we must rely on empirical equation (1).

Taillandier et al.⁴⁵ propose formulations of A , B and Δt that depend on temperature and on the initial SSA of the snow, SSA_0 . They propose two sets of parameterizations, one for QIM conditions (temperature gradient $<10^\circ\text{C.m}^{-1}$) and one for HGM conditions, (gradient $>20^\circ\text{C.m}^{-1}$). Taillandier et al. observed that the value of the temperature gradient did not affect the rate of SSA decrease, as long as it was above the 20°C.m^{-1} threshold.

Using the equations of Taillandier et al., we show (Figure 2) that a rise in temperature, at constant temperature gradient, accelerates SSA decrease, therefore decreasing the time-averaged SSA. However, climate warming will lead to a decrease in the temperature gradient in the snowpack, that may be amplified by increased snowpack thickness due to enhanced precipitation in polar regions (see Fig. 19 of Hansen et al.⁴⁸). The possibility thus exists that in some areas, the metamorphic regime will change from HGM to QIM. Figure 2 indeed shows that, except for the first day after the snowfall, the snow SSA remains higher under the warmer QIM conditions than under the colder HGM conditions.

Climate warming will therefore have a complex effect on snow SSA and therefore albedo. Warming without a change in metamorphic regime from HGM to QIM will decrease snow SSA, while warming with a change from HGM to QIM conditions will increase snow SSA. Moreover, an increased frequency of melting events will form melt-freeze crusts on the surface that have a very low SSA, so that the physical aspect of the climate warming-snow albedo feedback is very complex and will certainly show large geographical variations, both in magnitude and sign. These feedbacks can have large magnitudes, as estimated below.

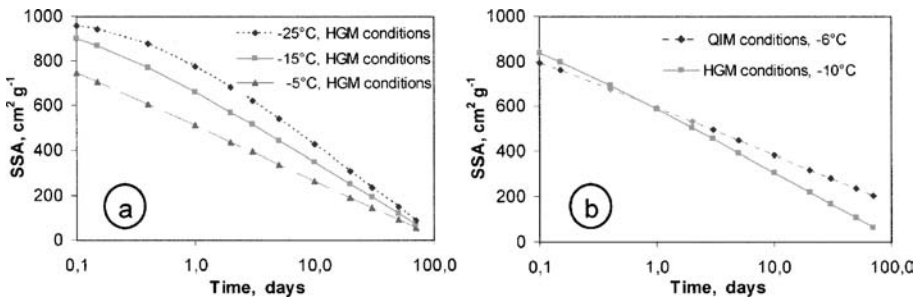


Figure 2 (a) Calculated rate of decrease of the specific surface area (SSA) of snow of initial SSA $1000 \text{ cm}^2 \text{g}^{-1}$ evolving under a temperature gradient greater than 20°C.m^{-1} (HGM conditions, see text) at three different temperatures. (b) *ibid.*, for snow evolving under two different conditions : quasi isothermal (QIM, see text) conditions at -6°C and under a temperature gradient greater than 20°C.m^{-1} (HGM conditions) at -10°C . This shows that after one day, a change in metamorphic regime from HGM to QIM offsets a warming of 4°C and SSA will then decrease slower under a warmer climate.

Several models have quantified the climate warming-snow albedo feedbacks caused by an increase in soot in polar snow. Hansen and Nazarenko¹⁸ found that predicted soot increases would decrease the spectrally-averaged albedo by 1.5%. This results in a 1.5 W.m^{-2} forcing at high latitude, producing a warming between 1 and 2°C .

Following the scenario of Figure 2b, we assume that climate-induced changes in snow metamorphism will increase snow SSA from 100 to $200 \text{ cm}^2 \text{g}^{-1}$. Using the method of

Stamnes et al.³⁶ we calculate that this will increase the spectrally-averaged snow albedo by 4% (from 0.75 to 0.79). With an incident solar flux of 100 W.m^{-2} , and assuming that the relationship between forcing and warming of Hansen and Nazarenko¹⁸ is linear, we predict that changes in snow physics will produce a cooling of 3 to 5°C . A slightly different parameterization⁴⁸ leads to a similar range : 2.5 to 4°C , still a significant cooling.

If fine-grained snow of $\text{SSA } 200 \text{ cm}^2.\text{g}^{-1}$ is replaced by a melt-freeze crust of $\text{SSA } 20 \text{ cm}^2.\text{g}^{-1}$, the reverse would be true and a positive feedback of 3 to 5°C would be produced. From Figure 2a, we predict that more limited positive feedbacks will be produced by a 5°C warming without a change in metamorphic regime, of the order of 1°C .

These considerations warrant further investigation but they show that the snow-albedo physical feedback, via SSA changes, can be strong. The extreme feedback strengths of 4 to 5°C , warming or cooling, are probably reserved to exceptional conditions and the sign of the feedback will probably vary with time and space, so that the overall effect of the warming-SSA feedback cannot be determined. We wish to stress, however, that snow-climate feedbacks may not all be positive, and that the climate-SSA feedback may be important and deserves investigations.

Changes in SSA will affect light penetration in the snowpack. The light extinction coefficient depends on $\text{Sc}^{1/2}$, and therefore on $\text{SSA}^{1/2}$.³⁹ If the SSA increases from 100 to $200 \text{ cm}^2.\text{g}^{-1}$, the e-folding depth and the light intensity integrated over the whole snowpack will decrease by a factor of 1.4.

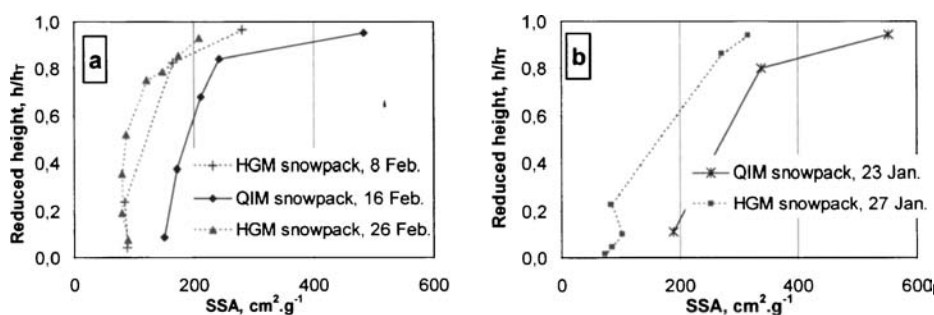


Figure 3 Measured snow SSA profiles in central Alaska in two different snowpacks : a natural snowpack on the ground, where a strong temperature gradient led to depth hoar formation (HGM snowpack); and the same snowpack on Tables, under which the air circulation prevented the establishment of a significant temperature gradient (QIM snowpack). (a) comparison of the QIM snowpack of 16 February with the HGM snowpack sampled 8 days before and 10 days after; (b) comparison of both snowpacks sampled just 4 days apart. In both cases the SSA is much higher in the QIM snowpack. Typical snowpack heights were 50 cm for HGM and 40 cm for QIM.

Our suggestion that an increase in snow SSA will result from a reduction in the temperature gradient was confirmed by field studies in Alaska during the 2003-2004 winter. Figure 3 compares the SSA evolution of the natural taiga snowpack to that of a snowpack where the temperature gradient was suppressed by allowing falling snow to accumulate on tables, under which air circulation prevented the establishment of a

temperature gradient. Until March, low insolation at our 65°N site limited surface heating and transient surface temperature gradients. In the natural snowpack on the ground, the temperature gradient reached 100°C.m⁻¹ in the fall, decreasing to 20°C.m⁻¹ in late winter. In the snowpack on the tables, the gradient mostly remained below 10°C.m⁻¹. Sampling and measurements were done alternatively on the ground and on the tables. Figure 3a clearly shows that the SSA vertical profile in the QIM snowpack on the tables displays higher values than both profiles in the HGM snowpack on the ground. Figure 3b shows samplings done just 4 days apart and the conclusion is the same. In most cases, values on the ground are a factor of 1.5 to 2 lower than on the tables, in reasonable agreement with Figure 2. This confirms that negative snow-climate feedback loops may exist.

Regions where this negative feedback may be observed include the southern edge of the taiga, where depth hoar formation may be reduced by warming and this may be enhanced by increased precipitation in the southern taiga of Canada and Eastern Siberia.⁴⁸ Other regions concerned by this effect may be the colder Alpine areas in the fall, when depth hoar formation will be hindered and conditions become more maritime-like. On the contrary, positive feedbacks are to be expected in the maritime and the warmer Alpine snowpacks, due to more frequent melting and to a faster SSA decrease under the QIM regime. Likewise, warming in the tundra and Northern taiga, without a change in metamorphic regime, is expected to enhance SSA decrease. The transformation of the southern tundra into shrub tundra and taiga¹⁹ may transform the tundra windpack into faceted crystals or depth hoar of lower SSA, leading to a decreased albedo and longer e-folding depth. The impact of the changing vegetation on the light intensity reaching the snow surface would also have to be accounted for, for a full quantification of effects.

Other factors may further complicate the climate-SSA feedback. Albedo is mostly determined by surface snow, although underlying layers also have an effect.⁴⁹ A critical factor to determine snow SSA is the age of the surface snow, and hence the time elapsed between snow falls. Thus, the time distribution of precipitation events, as well as that of wind storms, is an extra factor to consider when modeling the warming-albedo feedback.

3.3 Heat conductivity

The heat conductivity of snow, k_T , relates the vertical heat flow q through the snowpack to the temperature gradient dT/dz , where z is the vertical coordinate⁵⁰:

$$q = -k_T \frac{dT}{dz} \quad (2)$$

Values of k_T for dry snow vary by a factor of 25 from 0.026 to 0.65 W m⁻¹ K⁻¹.⁵⁰ The range is large because heat conduction in snow results from several processes (Figure 4) and the contribution of each process depends on the snow type, determined by metamorphism. For example, the most efficient process is conduction through the interconnected network of ice crystals. Depth hoar crystals are poorly interconnected and this snow type has the lowest k_T values, 0.026 to 0.10 W.m⁻¹.K⁻¹. Hard windpacks have strongly connected crystals and display the highest values for snows not subjected to melting, up to 0.65 W.m⁻¹.K⁻¹. Fined-grained snow that forms in temperate regions also have high k_T values, 0.3 to 0.4 W.m⁻¹.K⁻¹.

Climate change will modify k_T values in complex ways. Warming will limit depth hoar formation, increasing k_T . More frequent melting events in temperate climates will form ice layers with high k_T values. In contrast, the growth of shrubs on the tundra will limit the effect of wind,¹⁹ transforming windpacks into depth hoar of much lower k_T values.

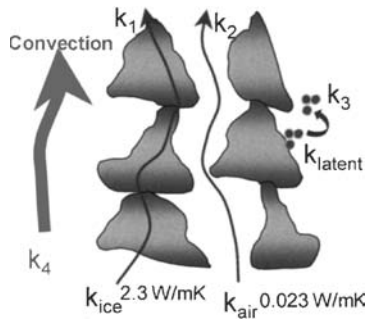


Figure 4 The main processes contributing to the heat conductivity of snow, k_T :
 k_1 =conduction through the network of interconnected ice crystals.
 k_2 =conduction through the air in the pore spaces.
 k_3 =latent heat transport across pore spaces due to ice condensation/sublimation cycles during metamorphism.
 k_4 =air convection in the pore space.

The heat conductivity of snow will therefore change in many areas, affecting ground temperature, permafrost extent and sea ice growth. Resulting effects on climate include:

- Change in microbial activity and in CO_2 and CH_4 emissions by soils.⁵¹
- Change in the duration of the snow cover, in the duration of the growing season and of carbon sequestration by the terrestrial biosphere.⁵²
- Modification of sea ice growth and areal extent and thus of the albedo of polar oceans.

To illustrate the climatic potential of changes in snow k_T values, we develop here the example of sea ice growth, based on observations and measurements on Storffjord, on the East coast of Spitzbergen during the winters of 2005 and 2006. While many effects intervene in sea ice growth,^{2,53,54} our objective is to use a simplified system to isolate the effect of changes in snow k_T . Our campaign site was perfect for this purpose: it was on fast ice, in a shallow sheltered bay with homogeneous sea ice and snow cover over more than 1 km in all directions, justifying the use of a 1-D model. In that bay, heat transport by oceanic current is greatly reduced and is neglected here. We measured sea ice thickness, snow stratigraphy and heat conductivity, and perform calculations using 2 temperature scenarios differing on average by 5.7°C (Figure 5a) : a cold one and a warm one, based on the unusually warm 2006 winter. Other simplifying assumptions are :

- The initial system consists of an ice layer 10 cm thick, over an isothermal ocean at the freezing temperature of sea ice, -1.8°C , on 1st October.
- The temperature was kept constant for a given month, at the values shown in Figure 5a.
- The snow stratigraphy was also kept constant for a given month.
- Given this lack of temperature variations, steady state was assumed, i.e. heat storage in snow and ice is negligible.
- All heat exchanges at the water/ice interface are latent heat. The value of latent heat used is that of pure ice : $3,3 \cdot 10^8 \text{ J.kg}^{-1}$.
- The temperature of the snow surface is equal to the air temperature.
- The heat conductivity of sea ice used is $2.1 \text{ W.m}^{-1}.\text{K}^{-1}$.⁵⁵

Under these conditions, the heat fluxes, q , at the air-snow and sea ice-ocean interfaces are always equal and are simply related to h_i , the thickness of snow or ice layer i , and to k_{Ti} , the heat conductivity of layer i by :

$$q = (T_{ocean} - T_{air}) / \sum_i h_i / k_{Ti} \quad (3)$$

Besides temperature (Figure 5a), the cold and warm scenarios differ by the structure of the snowpack. In both cases, the snow water equivalent have the same temporal evolution : 2 cm at the end of October, 11 cm at the end of January and 15.7 cm in late April. Stratigraphies and heat conductivities are very different. In the cold scenario, depth hoar layers of low densities (0.21 to 0.26 g.cm^{-3}) alternate with denser windpacks (0.38 to 0.48). Transient layers of fresh snow and of faceted crystals are also present. k_T values range from $0.06 \text{ W.m}^{-1}.\text{K}^{-1}$ for aged depth hoar to $0.46 \text{ W.m}^{-1}.\text{K}^{-1}$ for dense windpacks. In the warm scenario, two melt-freeze layers (densities 0.40 to 0.55) alternate with hard windpacks (0.34 to 0.41) while layers of fresh snow are sometimes included in the mean monthly stratigraphies. k_T values are 0.45 and $0.63 \text{ W.m}^{-1}.\text{K}^{-1}$ for the melt-freeze layers and range from 0.36 to $0.48 \text{ W.m}^{-1}.\text{K}^{-1}$ for dense windpacks. Recent snow has values around $0.2 \text{ W.m}^{-1}.\text{K}^{-1}$. Overall, the warm snowpack has a greater heat conductivity than the cold one.

Results are shown in Figure 5b. At the end of April, the ice thickness is 37 cm with the cold scenario and 58 cm with the warm scenario, so that changes in snow k_T more than offset atmospheric warming. This increased sea ice thickness clearly constitutes a negative snow-climate feedback loop that deserves consideration in climate models. Of course, this fast ice example cannot be taken at face value, as sea ice growth is much more complex than described here. Other effects must be taken into account such as convection in the water that depend on growth rate,⁵³ lateral heat fluxes in the ice and turbulent fluxes at the snow-air and sea-ice interfaces.^{2,54} However, this example does illustrate the importance of one factor, the heat conductivity of snow, that will be affected by climate change.

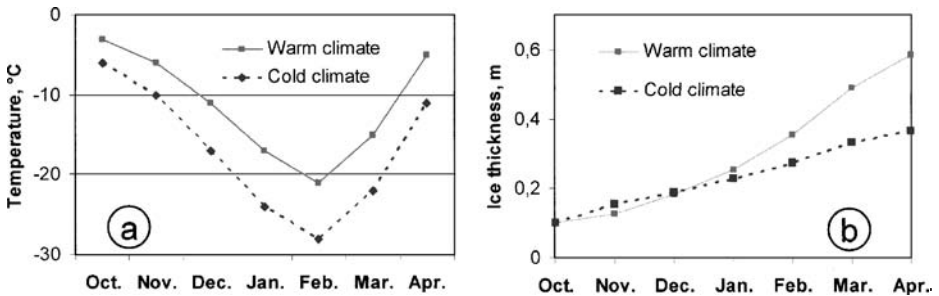


Figure 5 (a) Mean monthly average temperatures of the warm and cold temperature scenarios used to calculate sea ice growth. In the warm scenario, spells above freezing formed melt-freeze crusts and different snow stratigraphies and heat conductivities were used for each scenario (see text). (b) Ice thicknesses during the winter according to the warm and cold scenarios. At the end of winter, sea ice is thicker under the warm scenario, because of the higher k_T values.

3.4 Permeability

The snowpack is a porous medium through which air flows if pressure differences exist within the snowpack. Such pressure gradients may be generated by the action of wind on sastrugi. Under most conditions relevant to snowpacks, the flow velocity v is proportional to the pressure gradient $\partial P / \partial x$ and the proportionality factor is the snow permeability K_p divided by the air viscosity η (Darcy's law) :

$$v = - \frac{K_p}{\eta} \frac{\partial P}{\partial x} \quad (4)$$

The permeability of snow ranges from $20 \times 10^{-10} \text{ m}^2$ to about $500 \times 10^{-10} \text{ m}^2$ and is strongly dependent on snow type : it is highest for depth hoar, which has large crystals and a low density, and lowest on windpacks, that have small crystals and a high density.⁵⁶ Shimizu⁵⁷ proposed an empirical relationship to relate K_p (in m^2) to snow density ρ_s (in kg.m^{-3}) and grain diameter D (in m):

$$K_p = 0.077 e^{-0.0078\rho_s} D^2 \quad (5)$$

During metamorphism, grain size increases faster under high temperature gradients and culminates with centimetric depth hoar crystals in the taiga snowpack.²² A decrease in temperature gradient caused by global warming will therefore reduce grain size. Furthermore, upward vapor fluxes that compensate densification will also be reduced under a lower gradient. Slower crystal growth and a higher density caused by warming will therefore combine to reduce snow permeability. This prediction was confirmed by our field experiments in Alaska, described two sections up, where we compared the evolution of a given snowpack under a temperature gradient and under quasi-isothermal conditions.

In the natural snowpack on the ground, evolving under HGM conditions, depth hoar of density 0.20 g.cm^{-3} formed rapidly and the permeability in the lower half of the snowpack increased to beyond $500 \times 10^{-10} \text{ m}^2$ in late March. In contrast, on the tables under QIM conditions, fine-grained snow of density 0.28 g.cm^{-3} formed and the permeability decreased to values between 30 and $70 \times 10^{-10} \text{ m}^2$ in early March.

Warming will also increase the occurrence of melting events that produce melt/freeze crusts of low permeability. We therefore suggest that in most cases, climate change will result in a decrease in snow permeability. Of course, as mentioned above, in the southern tundra vegetation growth will reduce the effect of wind and facilitate depth hoar formation, enhancing snow permeability. But overall, the lower permeability induced by warming will reduce air flow through snow and therefore reduce the impact of one heat transfer process. This may partly counterbalance the increase in heat conductivity discussed earlier. However, the effect will be felt only in regions where highly permeable snow forms, essentially the taiga, where there is little wind. We do not attempt to quantify this thermal effect here but we suspect that it will be small. Its main impact may be on the transfer of chemical species from the snowpack to atmosphere, as discussed in the next chapter.

4 CHEMICAL PROPERTIES OF THE SNOWPACK

4.1 Chemical species in the snowpack

Species analyzed in snow include mineral and organic ions,^{58,59} organic molecules such as aldehydes, peroxides, pesticides and hydrocarbons,⁶⁰⁻⁶³ organic macromolecules present as particles⁶⁴ and mineral dust.³² Motivations for these analyses include the understanding of the quality of water resources and the interpretation of ice core analyses.⁶ Recently it has also become clear that snow is a complex multiphase (photo)chemical reactor producing species such as aldehydes, nitrogen oxides and halocarbons that impact atmospheric composition and reactivity.^{3,12,65,66} Atmospheric chemistry interacts with climate, so that a full treatment of snow-climate feedbacks must discuss snowpack chemical reactivity and how climate-induced changes in snow metamorphism will affect it. We first briefly discuss how chemical species are incorporated in snowpacks and how this affects their reactivity. We then speculate on how each type of reactivity is affected by climate change. The mechanisms through which snow can incorporate chemical species (Figure 6) include :

- **Adsorption.** The concentration of adsorbed species in snow is determined by snow SSA, temperature and by the partial pressure of the species in snowpack interstitial air.^{25,67,68} Thus, the reduction in SSA usually observed during metamorphism will lead to the emissions of adsorbed species. Adsorbed species are also readily available for dark and light-induced chemical reactions.⁶⁹
- **Formation of a solid solution.** Small molecules such as HCl, HNO₃, HCHO and H₂O₂ dissolve within the ice lattice to form a solid solution.^{10,61,70-73} The reactivity of these molecules will be limited by their trapping in the ice lattice. For example, photofragmentation will often lead to recombination through cage effects. Physical release will require solid state diffusion or sublimation during metamorphism.
- **Trapping of aerosol particles.** Falling snow efficiently scavenges particles suspended in air.⁷⁴ Wind blowing over snow also deposits particles within the snow, that acts as an efficient filter.^{16,17,75} The fate of these particles is not well known. Hydrophilic particles such as sulphate aerosols may interact with the snow and spread on the surface, but this is not documented. Some particles remain essentially unaffected, as observed by SEM⁷⁶ and just sit on the surface of snow crystals.

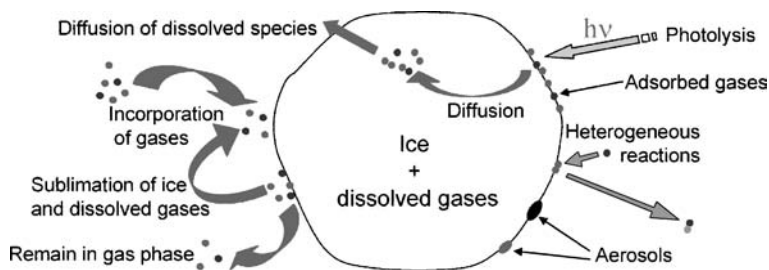


Figure 6 Location of impurities in snow and the mechanisms through which they can react and/or be released to snowpack interstitial air.

4.2 Adsorption/desorption of species

Modeling air-snow exchange of adsorbed species such as volatile and semi-volatile organic molecules requires the understanding of the rate of decrease of snow SSA,⁶⁸ that depends on temperature and on whether the snowpack is quasi-isothermal (QIM, temperature gradient $<10^{\circ}\text{C.m}^{-1}$) or under a high temperature gradient (HGM, gradient $>20^{\circ}\text{C.m}^{-1}$). Between these two values, data is lacking but a transition regime is likely.

Since both albedo and gas adsorption depend on SSA, the climate response of the concentration of species adsorbed within the snowpack will be similar to that of albedo : increase in regions where warming is accompanied by a change from HGM to QIM, such as the southern taiga and the warmer Alpine areas in the fall and decrease in the other regions. These effects will be modulated by the temperature increase, that will decrease the concentration of adsorbed species. For example, a temperature rise from -15 to -10°C will desorb 40% of adsorbed acetone molecules, that have an adsorption enthalpy of 57 kJ/mol ,⁶⁷ at constant SSA. The combined effect of warming and SSA change will then probably lead to a decrease in the concentration of adsorbed species in most areas.

4.3 Species forming a solid solution

In general, the concentration of soluble species in snow such as HCHO has been found to decrease with time.^{9,61} A hypothesis for this is that they are incorporated out of equilibrium in clouds, possibly because snow crystals there grow fast and solute concentration is governed by kinetics rather than equilibrium.^{70,77} Another possibility is that temperature and the partial pressure of the solute are very different in the cloud and at the surface, and re-equilibration takes place. Due to a lack of chemical measurements in clouds, it is difficult to test this hypothesis. In any case, since soluble species are usually emitted after precipitation, we will discuss how warming may affect emissions of these species.

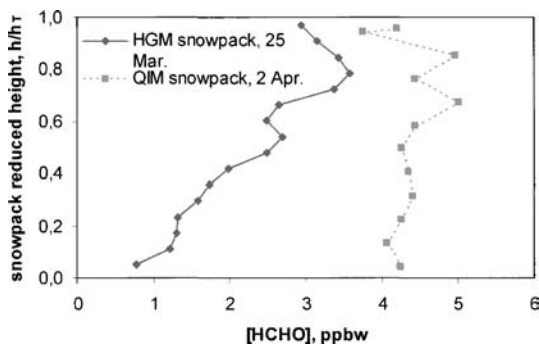


Figure 7 Vertical profiles of formaldehyde, HCHO , in the snowpacks in central Alaska described in Figure 3 and subjected to different thermal regimes : a temperature gradient (HGM) regime, and a quasi-isothermal (QIM) regime.

Warming will reduce the temperature gradient in the snowpack and the intensity of sublimation/condensation cycles that are the most likely to lead to the release of ice-

soluble species. We then propose that emissions will decrease in a warmer climate. To test this idea, HCHO was measured during the Alaska field experiment described above, where two snowpacks were compared : one with the natural temperature gradient (HGM) and one where this gradient had been suppressed (QIM). Results (Figure 7) clearly demonstrate that emissions were suppressed in the QIM snowpack, as deeper layers retain their initial concentrations, while most of the HCHO is eventually lost from the HGM snowpack. We then suggest that in many cases (except again in the southern tundra) warming will limit the release of ice-soluble species to the atmosphere by ice sublimation. This effect may however be counterbalanced by increased diffusion rates at higher temperature, enhancing release.⁹ Soluble species such as HCHO and H₂O₂ are oxidant precursors, as their photolysis releases HO_x radicals. These processes may then modify the oxidative capacity of the atmosphere over snow-covered regions. They therefore deserve attention.

4.4 Photochemical reactions

Many reactive species emitted by the snowpack such as NO, NO₂, HONO, aldehydes, alkenes and hydrocarbons^{12,13,64-66,78} are produced by photochemical reactions. Photochemistry also produces species that are not volatile enough to be emitted to the atmosphere, such as complex hydrocarbons,⁶⁹ but these will modify snow and ice core chemistry and this aspect therefore also has interest. The rate of photochemical production is proportional to the light flux inside the snowpack. As detailed above, this will be inversely proportional to SSA^{1/2}. Similarly to the discussion in section 3.2, we speculate that a temperature increase without change in metamorphic regime will increase the rate of SSA decrease and therefore increase the light flux in the snow and photochemical production in the snowpack. Warming with a concomitant change of metamorphic regime will on the contrary decrease snowpack photochemical production.

4.5 Emissions of species from interstitial air

Species emitted to snowpack interstitial air must be transported out of the snow into the atmosphere to have an atmospheric impact. The most efficient mechanism is ventilation by wind, which depends on wind speed, snow surface structure and permeability. Hansen et al.⁴⁸ predict little surface wind change in polar regions. Snow surface structure depends mostly on wind, but speculating on its evolution is beyond our scope. We discussed that snow permeability will in general decrease with warming. The residence time of species produced in interstitial air will therefore increase under a warmer climate, reducing the chances of reactive species to escape before they react in the snowpack.

For example, HCHO and H₂O₂ can photolyze and the HO_x radicals produced can react with organic species contained in aerosols that are always present in snow. Other species will be produced,⁶⁴ that can also be released to the atmosphere, so that the nature of snowpack emissions are highly dependent on the residence time of primary products in the snowpack. Complex snow photochemical models, inexistent today, are needed to predict the effect of warming on snowpack emissions, caused by changes in snow permeability.

4.6 Overall climate-chemistry interactions

It is then clear that we lack critical data and understanding to predict with confidence how warming will affect snowpack chemical emissions to the atmosphere. It does appear, however, that in regions where both warming and a change in metamorphic regime will take place, most processes will lead to reduced emissions : reduced emissions of adsorbed

species because of a slower SSA decrease, reduced photochemical activity because of the reduced light flux caused by the slower SSA decrease, slower release of dissolved species because of a reduced metamorphic intensity and slower transfer from the snowpack air to the atmosphere due to a decrease in permeability, although the impact of this last aspect is far from clear. Following previous discussions, such a scenario may take place at the southern edge of the taiga and in warmer Alpine snowpacks in the fall.

In regions where warming will not lead to a change in metamorphic regime, many antagonistic effects will take place. SSA will decrease faster, leading to enhanced desorption and photochemical activity. On the contrary, the reduced metamorphic intensity due to decreased temperature gradients will lead to lower emissions of dissolved species and slower transfer from snowpack air to the atmosphere, so that the net effect is at present unpredictable. This scenario will probably be seen in the northern taiga, in the colder Alpine areas and in the tundra that is not transformed into taiga by warming and the northern migration of vegetation zones.

If the southern tundra turns into shrub tundra or taiga¹⁹ the transformation of the tundra windpack into faceted crystals or depth hoar of lower SSA, longer e-folding depth and higher permeability will lead to enhanced release of adsorbed and dissolved species, greater photochemical activity (modulated by tree shading) and more efficient release to the atmosphere, so that emissions may in this case increase.

In summary, the spatially-resolved prediction of how warming will affect chemical emissions by snow will probably need the coupling of a general circulation model to a photochemical model and to a vegetation model. Building a snow photochemical model would need new developments and more importantly, an improved understanding of the location of species in the snowpack. Quantifying the chemistry-climate feedback will furthermore require the coupling of these models with an atmospheric chemistry model.

5 CONCLUSION

The ideas proposed here and the data shown indicate that snow will exert many physical and chemical feedbacks on climate change. Most snow-climate feedbacks considered so far, such as the decrease in the areal extent of snow coverage,⁴ the increase of soot in snow¹⁸ and climate-vegetation-snow interactions,¹⁹ are positive feedbacks. Here we investigate other feedbacks, such as the snow albedo-climate feedback and the snow heat conductivity-climate feedback, to conclude that their sign and magnitude will show large spatial and temporal variations, so that complex modeling is needed to quantify them. Our considerations, that have a large speculative character, suggest that significant negative climate feedbacks may take place in the southern taiga and in the warmer Alpine snowpack in the fall, while the tundra and Northern taiga will experience mostly positive feedbacks. The case of sea ice is interesting. A very simplified 1-D model suggests that in some areas, changes in the heat conductivity of snow may contribute to increased ice growth. Quantifying the overall effect of warming on ice growth must however also take into account many other complex effects.

The complexity of snow-climate feedbacks is illustrated by the observations that increases in atmospheric temperatures on the one hand and of snowpack and sea ice areal extents on the other, are not well correlated. Temperature has risen almost continuously, although at variable rates, since the beginning of the 20th century.⁷⁹ However, until the early 1980's, snow areal and temporal coverages have increased in most areas in the Northern hemisphere and a significant decrease has started to be observed only after that date.⁸⁰⁻⁸² Regarding sea ice, the signal is complex, with no significant trend in Antarctica,

while the Arctic has seen a recent decrease.⁴ These observations confirm that poorly identified and complex feedbacks may be at work. Elucidating them will require new model developments, the coupling of several models and perhaps more importantly, new observations that will produce time series of several physical and chemical properties of the snowpack, averaged over large areas. This is necessary to parameterize and test complex models. Setting up snow observatories would greatly assist in this enterprise.

Acknowledgements

F. Domine thanks the organizers of PCI 2006 for their kind invitation. Snow physics data obtained in Alaska was supported in part by the Chapman chair (Pr. Norbert Untersteiner) and by the International Arctic Research Center. The formaldehyde profiles were obtained by the FAMAS program funded by the French Polar Institute (IPEV) to S. Houdier. The Spitzbergen observations that inspired Figure 5 were funded by IPEV through the OSMAR program to F. Domine. Helpful comments by M. Sturm are gratefully acknowledged.

References

- 1 T. Zhang, *Rev. Geophys.*, 2005, **43**, RG4002. doi: 10.1029/2004RG000157.
- 2 M. Sturm, D.K. Perovich, and J. Holmgren, *J. Geophys. Res.*, 2002, **107**, 8047, doi: 10.1029/2000JC000409.
- 3 F. Dominé and P.B. Shepson, *Science*, 2002, **297**, 1506.
- 4 R.A. Pielke, G.E. Liston, W.L. Chapman and D.A. Robinson, *Climate Dynamics*, 2004, **22**, 591.
- 5 S.C. Colbeck, *Rev. Geophys. Space Phys.*, 1982, **20**, 45.
- 6 M. Legrand and P. Mayewski, *Rev. Geophys.* 1997, **35**, 219.
- 7 F. Dominé, E. Thibert, E. Silvente, M. Legrand, and J.-L. Jaffrezo, *J. Atmos. Chem.*, 1995, **21**, 165.
- 8 K. Nakamura, M. Nakawo, Y. Ageta, K. Goto-Azuma and K. Kamiyama, *Bull. Glaciol. Research*, 2000, **17**, 11.
- 9 Perrier, S., Houdier, S., F. Dominé, A. Cabanes, L. Legagneux, A.L. Sumner, P.B. Shepson, *Atmos. Environ.*, 2002, **36**, 2695.
- 10 M.A. Hutterli, J.R. McConnell, G. Chen, R.C. Bales, D.D. Davis and D.H. Lenschow, *Atmos. Environ.*, 2004, **38**, 5439.
- 11 W.R. Simpson, M.D. King, H.J. Beine, R.E. Honrath and X. Zhou, *Atmos. Environ.*, 2002, **36**, 2663.
- 12 A.L. Sumner and P.B. Shepson, *Nature*, 1999, **398**, 230.
- 13 R. Honrath, M.C. Peterson, Y. Lu, J.E. Dibb, M.A. Arsenault, N.J. Cullen and K. Steffen, *Atmos. Environ.*, 2002, **36**, 26290.
- 14 R.A. Schmidt, *Boundary-layer Meteorol.*, 1986, **34**, 213.
- 15 J.W. Pomeroy and L. Li, *J. Geophys. Res.*, 2000, **105**, 26619.
- 16 T. Aoki, T. Aoki, M. Fukabori, A. Hachikubo, Y. Tachibana and F. Nishio, *J. Geophys. Res.*, 2000, **105D**, 10219.
- 17 F. Dominé, R. Sparapani, A. Ianniello and H. J. Beine, *Atm. Chem. Phys.*, 2004, **4**, 2259.
- 18 J. Hansen and L. Nazarenko, *Proc. Nation. Acad. Sci.* 2004, **101**, 423.
- 19 M. Sturm, J.P. McFadden, G.E. Liston, F.S. Chapin, C.H. Racine and J. Holmgren, *J. Climate*, 2001, **14**, 336.
- 20 M. Kanakidou et al. *Atmos. Chem. Phys.*, 2005, **5**, 1053.
- 21 S.C. Colbeck, *J. Geophys. Res.*, 1983, **88**, 5475.

- 22 M. Sturm and C.S. Benson, *J. Glaciol.*, 1997, **43**, 42.
- 23 F. Dominé, T. Lauzier, A. Cabanes, L. Legagneux, W.F. Kuhs, K. Techmer and T. Heinrichs, *Microsc. Res. Tech.*, 2003, **62**, 33.
- 24 M. Sturm, J. Holmgren, and G. Liston, *J. Climate*, 1995, **85**, 1261.
- 25 F. Dominé, A. Cabanes and L. Legagneux *Atmos. Environ.*, 2002, **36**, 2753.
- 26 J.B. Brzoska, B. Lesafre, C. Coléou, K. Xu and R.A. Pieritz, *Eur. Phys. J. AP.*, 1999, **7**, 45.
- 27 D. Marbouty, *J. Glaciol.*, 1980, **26**, 303.
- 28 E. Brun, P. David, M. Sudul and G. Brunot, *J. Glaciol.*, 1992, **128**, 13.
- 29 R.A. Schmidt, *Boundary-layer Meteorol.*, 1982, **23**, 223.
- 30 F. Domine, R. Salvatori, L. Legagneux, R. Salzano, M. Fily and R. Casacchia, *Cold Regions Sci. Technol.*, 2006, **46**, 60.
- 31 L. Legagneux, A. Cabanes and F. Dominé, *J. Geophys. Res.*, 2002, **107D**, 4335, doi:10.1029/2001JD001016.
- 32 T.C. Grenfell, S. G. Warren and P. C. Mullen, *J. Geophys. Res.*, 1994, **99**, 18669.
- 33 S.G. Warren, *Rev. Geophys. Space Phys.*, 1982, **20**, 67.
- 34 T.C. Grenfell, B. Light, and M. Sturm, *J. Geophys. Res.*, 2002, **107**, C8032, doi:10.1029/2000JC000414.
- 35 W.J. Wiscombe, *The delta-Eddington approximation for a vertically inhomogeneous atmosphere*, NCAR Technical Note, NCAR/TN-121+STR, 1977, pp.1-66.
- 36 K. Stamnes, S.C. Tsay, W. Wiscombe and K. Jayaweera, *Applied Optics*, 1988, **27**, 2502.
- 37 T.C. Grenfell and S.G. Warren, *J. Geophys. Res.*, 1999, **104**, 31697.
- 38 S.P. Neshyba, T.C. Grenfell and S.G. Warren, *J. Geophys. Res.*, 2003, **108D**, 4448. doi: 10.1029/2002JD003302.
- 39 W.R. Simpson, G.A. Phillips, A.-S. Taillandier and F. Domine, in preparation.
- 40 F. Domine, A.-S. Taillandier and W.R. Simpson, *J. Geophys. Res.*, submitted.
- 41 A. Cabanes, L. Legagneux and F. Dominé, *Atmos. Environ.*, 2002, **36**, 2767.
- 42 A. Cabanes, L. Legagneux and F. Dominé, *Environ. Sci. Technol.*, 2003, **37**, 661.
- 43 L. Legagneux, T. Lauzier, F. Dominé, W.F. Kuhs, T. Heinrichs and K. Techmer, *Can. J. Phys.*, 2003, **81**, 459.
- 44 L. Legagneux, A.-S. Taillandier and F. Domine, *J. Appl. Phys.*, 2004, **95**, 6175.
- 45 A.-S. Taillandier; F. Domine, W.R. Simpson, M. Sturm and T.A. Douglas, *J. Geophys. Res.*, submitted.
- 46 L. Legagneux and F. Domine, *J. Geophys. Res.*, 2005, **110**, F04011. doi: 10.1029/2004JF000181.
- 47 M.G. Flanner and C.S. Zender, *J. Geophys. Res.*, 2006, **111**, D12208. doi:10.1029/2005JD006834.
- 48 J. Hansen et al., *J. Geophys. Res.*, 2005, **110**, D18104. doi:10.1029/2005JD005776.
- 49 X Zhou, S Li and K. Stamnes, *J. Geophys. Res.*, 2003, **108**, 4738. DOI: 10.1029/2003JD003859.
- 50 M. Sturm, J. Holmgren, M. König and K. Morris, *J. Glaciol.*, 1997, **43**, 26.
- 51 M.L. Goulden, J.W. Munger, S.-M. Fan, B.C. Daube and S.C. Wofsy, *Science*, 1996, **271**, 1576.
- 52 M. Stieglitz, A. Ducharme, R. Koster and M. Suarez, *J. Hydromet.*, 2001, **2**, 228.
- 53 T. Fichet, B. Tartinville and H. Goosse, *Geophys. Res. Lett.*, 2000, **27**, 401.
- 54 E.L. Andreas, R.E. Jordan and A.P. Makshtas, *J. Hydromet.* 2004, **5**, 611.
- 55 D.J. Pringle, H.J. Trodahl and T.G. Haskell, *J. Geophys. Res.* 2006, **111**, C05020. doi:10.1029/2005JC002990.
- 56 M.R. Albert and E. Shultz, *Atmos. Environ.*, 2002, **36**, 2789.

- 57 H. Shimizu, *Air permeability of deposited snow*, Institute of low temperature science, Sapporo, Japan, 1970 Contribution N° 1053. English translation.
- 58 J.E. Dibb, R.W. Talbot and M.H. Bergin, *Geophys. Res. Lett.*, 1994, **21**, 1627.
- 59 M. Legrand and M. De Angelis, *J. Geophys. Res.*, 1996, **101**, 4129.
- 60 S. Houdier, S. Perrier, F. Dominé, A.M. Grannas, C. Guimbaud, P.B. Shepson, H. Boudries and J.W. Bottenheim, *Atmos. Environ.*, 2002, **36**, 2609.
- 61 H.-W. Jacobi, M.M. Frey, M.A. Hutterli, R.C. Bales, O. Schrems, N.J. Cullen, K. Steffen and C. Koehler, *Atmos. Environ.*, 2002, **36**, 2619.
- 62 S. Villa, M. Vighi, V. Maggi, A. Finizio and E. Bolzacchini, *J. Atmos. Chem.*, 2003, **46**, 295.
- 63 J.-L. Jaffrezo, M.P. Clain and P. Masclet, *Atmos. Environ.*, 1994, **28**, 1139.
- 64 A.M. Grannas, P.B. Shepson and T.R. Filley, *Global. Biogeochem. Cycles*, 2004, **18**, GB1006.
- 65 H. J. Beine, R.E. Honrath, F. Dominé, W. R. Simpson and J. D. Fuentes, *J. Geophys. Res.*, 2002, **107D**, 4584, doi:10.1029/2002JD002082.
- 66 A.L. Swanson, N.J. Blake, D.R. Blake, F.S. Rowland and J.E. Dibb, *Atmos. Environ.*, 2002, **36**, 2671.
- 67 F. Dominé and L. Rey-Hanot, *Geophys. Res. Lett.*, 2002, **29**, 1873, doi:10.1029/2002GL015078.
- 68 G.L. Daly and F. Wania, *Environ. Sci. Technol.*, 2004, **38**, 4176.
- 69 J. Klanova, P. Klan, J. Nosek, I. Holoubek, *Environ. Sci. Technol.*, 2003, **37**, 1568.
- 70 F. Dominé and E. Thibert, *Geophys. Res. Lett.*, 1996, **23**, 3627.
- 71 E. Thibert and F. Dominé, *J. Phys. Chem. B.*, 1997, **101**, 3554.
- 72 E. Thibert and F. Dominé, *J. Phys. Chem. B.*, 1997, **102**, 4432.
- 73 S. Perrier, P. Sassin and F. Dominé, *Can. J. Phys.*, 2003, **81**, 319.
- 74 Y.D. Lei and F. Wania, *Atmos. Environ.*, 2004, **38**, 3557.
- 75 S. Harder, S.G. Warren and R.J. Charlson, *J. Geophys. Res.*, 2000, **105D**, 22,825.
- 76 C. Magano, F. Endoh, S. Ueno, S. Kubota and M. Itasaka, *Tellus*, 1979, **31**, 102.
- 77 F. Dominé and C. Rauzy, *Atm. Chem. Phys.*, 2004, **4**, 2513.
- 78 A.M. Grannas, P.B. Shepson, C. Guimbaud, A.L. Sumner, M. Albert, W. Simpson, F. Dominé, H. Boudries, J.W. Bottenheim, H.J. Beine, R. Honrath and X. Zhou, *Atmos. Environ.*, 2002, **36**, 2733.
- 79 IPCC, *Climate Change 2001: The Scientific Basis* J. T. Houghton, Y. Ding, D. J. Griggs, P. J. van der Linden, X. Dai, K. Maskell and C. A. Johnson, Eds., Cambridge University Press, 2001, 881 pp.
- 80 D.G. Dye, *Hydrol. Process.*, 2002, **16**, 3065.
- 81 H. Ye, *Geophys. Res. Lett.*, 2001, **28**, 551.
- 82 M. Laternser and M. Schneebeli, *Int. J. Climatol.*, 2003, **23**, 733. doi: 10.1002/joc.912